

# The Generation of Thermostable Fungal Laccase Chimeras by SCHEMA-RASPP Structure-Guided Recombination *in Vivo*

Ivan Mateljak,<sup>†</sup> Austin Rice,<sup>‡</sup> Kevin Yang,<sup>‡</sup> Thierry Tron,<sup>§</sup> and Miguel Alcalde<sup>\*,†,§</sup>

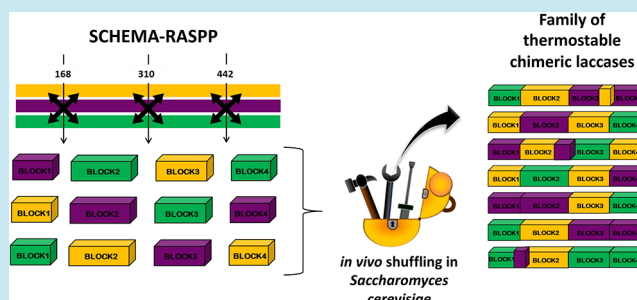
<sup>†</sup>Department of Biocatalysis, Institute of Catalysis, CSIC, Cantoblanco, 28049 Madrid, Spain

<sup>‡</sup>Division of Chemistry and Chemical Engineering, California Institute of Technology, CALTECH, Pasadena, California 91125-4100, United States

<sup>§</sup>Aix Marseille Université, Centrale Marseille, CNRS, iSm2 UMR 7313, 13397 Marseille, France

## Supporting Information

**ABSTRACT:** Fungal laccases are biotechnologically relevant enzymes that are capable of oxidizing a wide array of compounds, using oxygen from the air and releasing water as the only byproduct. The laccase structure is comprised of three cupredoxin domains sheltering two copper centers—the T1Cu site and the T2/T3 trinuclear Cu cluster—connected to each other through a highly conserved internal electron transfer pathway. As such, the generation of laccase chimeras with high sequence diversity from different orthologs is difficult to achieve without compromising protein functionality. Here, we have obtained a diverse family of functional chimeras showing increased thermostability from three fungal laccase orthologs with ~70% protein sequence identity. Assisted by the high frequency of homologous DNA recombination in *Saccharomyces cerevisiae*, computationally selected SCHEMA-RASPP blocks were spliced and cloned in a one-pot transformation. As a result of this *in vivo* assembly, an enriched library of laccase chimeras was rapidly generated, with multiple recombination events simultaneously occurring between and within the SCHEMA blocks. The resulting library was screened at high temperature, identifying a collection of thermostable chimeras with considerable sequence diversity, which varied from their closest parent homologue by 46 amino acids on average. The most thermostable variant increased its half-life of thermal inactivation at 70 °C 5-fold (up to 108 min), whereas several chimeras also displayed improved stability at acidic pH. The two catalytic copper sites spanned different SCHEMA blocks, shedding light on the recognition of specific residues involved in substrate oxidation. In summary, this case-study, through comparison with previous laccase engineering studies, highlights the benefits of bringing together computationally guided recombination and *in vivo* shuffling as an invaluable strategy for laccase evolution, which can be translated to other enzyme systems.



Laccases are versatile biocatalysts that belong to the group of blue multicopper containing oxidases. They harbor one T1Cu ion, where the oxidation of a wide range of substrates takes place, and a T2/T3 trinuclear Cu cluster, where molecular oxygen is reduced to water, while the whole protein structurally is arranged into three cupredoxin domains. Laccases have generated considerable interest in biotechnology, and they have been used in organic synthesis and in various industrial fields, from bioremediation, food and textiles, pulp-biobleaching, biofuel cells, and biosensor development.<sup>1,2</sup> Laccases are widely distributed in fungi, higher plants, and bacteria, performing a variety of biological activities. An important advantage of fungal laccases over their plant and bacterial counterparts is the high-redox potential at the T1Cu site. As such, high-redox potential fungal laccases (HRPLs) exhibit strong catalytic activity, oxidizing a broad spectrum of compounds with high-redox potential, including high-redox potential mediators, upon which medium- and low-redox potential laccases hardly act.<sup>3</sup> For years, the engineering of HRPLs has attracted much attention, mostly taking advantage

of a palette of library creation methods coupled to screening assays as part of different directed evolution campaigns.<sup>4</sup> These approaches have been aimed at enhancing heterologous expression and activity against different substrates, or at augmenting the stability of the enzyme in non-natural environments like organic solvents, ionic liquids, and human blood, to name but a few.

While laboratory evolution from individual fungal laccase templates have been successful, attempts to generate laccase chimeras from different orthologs have been less productive. For example, when we tried to combine two evolved HRPL versions—engineered for secretion in yeast—from *basidiomycetes* PM1<sup>5</sup> and *Pycnoporus cinnabarinus*<sup>6</sup> via *in vitro* and *in vivo* DNA shuffling, only a limited set of functional chimeras was obtained, with poor sequence diversity. That is, the chimeras were mostly composed of the highest-expressing parent with few crossover events in the mature protein.<sup>7</sup> Similarly, laccase

Received: December 4, 2018

Published: March 21, 2019

chimeras designed by *in vivo* shuffling of several isoforms in *S. cerevisiae* (Lac1, Lac2, Lac3, and Lac5 from *Trametes* sp. strain C30) generated a library prone toward the Lac3 parent due to its stronger expression in this heterologous host.<sup>8</sup> Moreover, preliminary rational design of chimeras was attempted with two isoforms (Lcc1 and Lcc4) from the basidiomycete *Lentinula edodes* expressed in tobacco By-2 cells, connecting the N-terminus of Lcc1 to the C-terminus of Lcc4 (*i.e.*, producing only one crossover point).<sup>9</sup> Due to the complex laccase structure, with two Cu centers connected to each other through a highly conserved HisCysHis tripeptide of 12 Å that regulates the flow of electrons between the two catalytic sites, it is difficult to obtain significant sequence diversity from chimeragenesis experiments without endangering protein function.<sup>10,11</sup>

SCHEMA structure-guided protein recombination is a computational method that is extremely useful to create chimeric proteins with large sequence diversity. This approach has been applied to cytochrome P450 monooxygenases,  $\beta$ -lactamases, cellulases, arginases, and channel rhodopsins, most notably to improve thermostability, but also substrate specificity, pH dependence, and membrane localization.<sup>12–20</sup> In structure-guided recombination, the crossover locations are selected in order to minimize disruption to the 3-dimensional protein structure, as measured by the library-average SCHEMA energy. The SCHEMA energy ( $E$ ) is the average number of pairwise interactions in a recombination library that are not present in any of the library parents.<sup>21</sup> To complement the SCHEMA method, Arnold's group also developed the RASPP (Recombination as Shortest Path Problem) algorithm to solve the problem of generating libraries that minimize ( $E$ ) for a range of ( $m$ )—the average number of mutations in a library relative to the closest parent, enabling functional chimeras to be created with greater sequence diversity.<sup>22</sup>

Here, we present a family of chimeric laccases obtained by SCHEMA-RASPP structure-guided recombination combined with *in vivo* shuffling in *S. cerevisiae*. Computationally designed SCHEMA blocks were introduced into *S. cerevisiae* where they were shuffled and assembled *in vivo* with the help of flanking overlapping areas specifically conceived at the crossover locations. The library of functional chimeras was designed from three high-redox potential fungal laccase orthologs, and it was screened at high temperatures. A family of chimeras was obtained with high sequence diversity derived from recombination events both between and within SCHEMA blocks, showing notably improved thermostability. Moreover, several of the chimeric laccases displayed modified activity preferences for particular substrates and enhanced stability at acidic pH. The library construction method that combined SCHEMA-RASPP with *in vivo* DNA recombination in yeast is discussed in depth, as are its implications in protein chimeragenesis.

## RESULTS AND DISCUSSION

**Departure Point: Parental Laccases.** Heterologous functional expression of HRPLs is difficult to achieve.<sup>4,23</sup> Indeed, the complex post-translational modifications (N-terminal and/or C-terminal processing, glycosylation) that laccases undergo along the secretory pathway, as well as the precise coordination of four copper ions at two distant sites, have precluded their functional expression in standard prokaryotic hosts like *Escherichia coli* or *Bacillus subtilis*. In eukaryotic hosts, some fine-tuning is typically needed to obtain reasonable levels of secretion. In previous work, we achieved

adequate expression in *S. cerevisiae* of two HRPLs from basidiomycetous PM1 (PM1L)<sup>5</sup> and *Pycnoporus cinnabarinus* (PcL)<sup>6</sup> by laboratory evolution. In both cases secretion was improved from scratch by switching the native laccase signal peptide to the  $\alpha$ -factor prepro-leader from *S. cerevisiae* ( $\alpha$ 1– $\alpha$ 89) and subjecting the corresponding fusions to iterative rounds of random mutagenesis and recombination. Through this approach, the secretion variants OB-1 (secreted at 8 mg/L and carrying the mutations V[ $\alpha$ 10]D-N[ $\alpha$ 23]K-A[ $\alpha$ 87]T-V162A-H208Y-S224G-A239P-D281E-S426N-A461T) and 3PO (secreted at 2 mg/L and carrying the mutations A[ $\alpha$ 9]D-F[ $\alpha$ 48]S-S[ $\alpha$ 58]G-G[ $\alpha$ 62]R-E[ $\alpha$ 86]G-N208S-R280H-N331D-D341N-P394H) were obtained from PM1L and PcL, respectively (the mutations lying in the evolved  $\alpha$ -factor prepro-leaders— $\alpha^{PM1}$  and  $\alpha^{PcL}$ —are underlined). In another study, the medium-redox potential Lac3 laccase isoform from the basidiomycete *Trametes* sp. strain C30 was expressed in *S. cerevisiae* at 2 mg/L by attaching the invertase leader sequence from yeast.<sup>24</sup> In the current study, OB-1, 3PO, and Lac3 were chosen as the departure points for laccase chimeragenesis. These orthologs shared roughly 70% sequence identity at the protein level, and they had a redox potential at the T1Cu site ranging from 680 to 790 mV vs NHE (Normal Hydrogen Electrode), as well as a half-life of thermal inactivation between 8 and 22 min (the half-life ( $t_{1/2}$ ) is defined as the incubation time at 70 °C that will reduce postincubation enzyme activity at room temperature by 50%, Table 1). To maximize parental enzyme secretion prior to

**Table 1. Comparison of Parental Laccases**

laccase	identity (%)			amino acids	$t_{1/2}^a$ (min)	$E_{T1}$ (mV) vs NHE
	OB-1	Lac3	3PO			
OB-1		69.96	72.98	496	22	740
Lac3	69.96		68.61	501	16	680
3PO	72.98	68.61		497	8	790

<sup>a</sup>The values of half time ( $t_{1/2}$ ) were obtained by measuring residual activity after enzyme incubation at 70 °C.

SCHEMA-RASPP, we designed 9 fusions to consider all the possible combinations of the different  $\alpha$ -factor prepro-leaders ( $\alpha^{native}$ ,  $\alpha^{PM1}$ , and  $\alpha^{PcL}$ ) for each of the three parental laccases,<sup>25</sup> Supplementary Figure S1. The invertase leader sequence was not included in this benchmarking as previous studies on PM1L and PcL discouraged its use. The evolved  $\alpha^{PcL}$  provided the strongest expression irrespective of the laccase to which it was attached, and therefore, it was used with the three parental variants to express and screen the SCHEMA library.

**SCHEMA-RASPP Library Design and Recombination *in Vivo*.** An ideal enzyme chimeragenesis experiment using SCHEMA is based on a three-step approach called “sample, model, and predict”:<sup>26</sup> step 1, SCHEMA family design; step 2, synthesis of a representative subset of SCHEMA sequences that are expressed functionally and characterized biochemically; and step 3, the prediction, through regression, of those chimeric sequences with the most desirable traits for their subsequent synthesis. This strategy has proved to be successful for many recombinant intracellular enzymes expressed in bacteria. However, the results for extracellular enzymes are less encouraging, as a subset of chimeras may not be easily secreted, compromising the representation of the SCHEMA

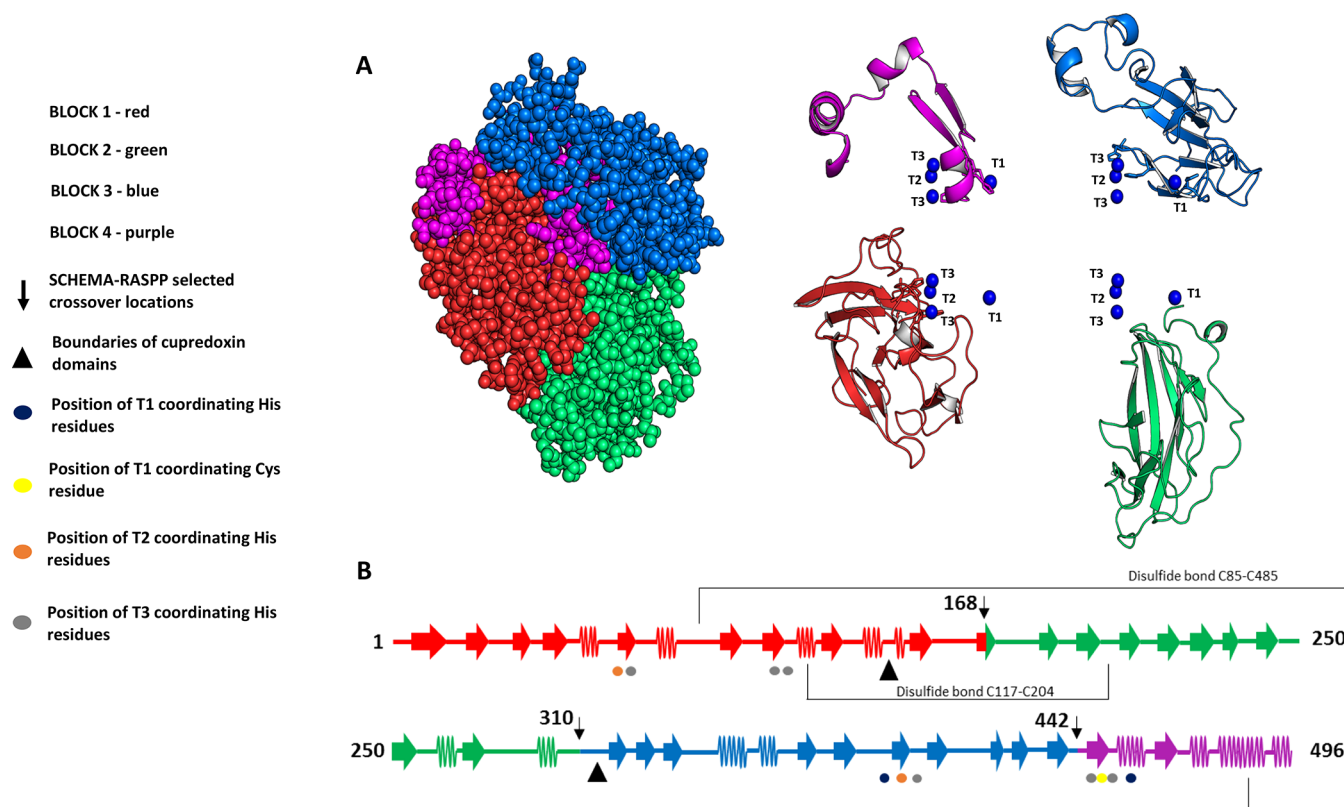


**Figure 1.** SCHEMA recombination library design. (A) The laccase structure is depicted as spheres and as a cartoon. Copper atoms are highlighted as blue spheres. The SCHEMA building blocks are shown in different colors. Model of the OB-1 laccase based on the high resolution structure of *Trametes trogii* laccase (PDB entry 2HRG), sharing 96% sequence identity to OB-1. (B) Secondary structure of SCHEMA blocks highlighted in different colors.

blocks in the sample.<sup>16</sup> In the case of our heavily glycosylated HRPLs, their poor secretion and complex structural architecture are attributes not well-suited to reliable linear regression modeling, which led us to SCHEMA library construction and screening. In previous studies, the combinatorial recombination of SCHEMA-defined gene fragments had been accomplished through time-consuming and expensive *in vitro* methods or DNA synthesis.<sup>27</sup> However, and even considering the progressive price drop in DNA synthesis, there is still an urgent need for reliable cloning and recombination methods, especially when one is faced with the challenge of screening thousands of clones per day.<sup>28,29</sup> For years, our favorite recombination strategy for eukaryotic genes has been based on the high-frequency homologous DNA recombination of *S. cerevisiae*, through which we have engineered different enzymes for a variety of processes.<sup>23</sup> As such, we took advantage of the recombination machinery of *S. cerevisiae* to shuffle and clone the SCHEMA blocks *in vivo* in a drive to enrich the functional diversity of the mutant library while maximizing the throughput of library generation.

We first modified the SCHEMA-RASPP algorithm by writing two scripts to give us additional information in order to select crossover points in areas of higher sequence identity between the three laccase orthologs that can then be used for recombination in yeast (see [Supporting Information](#)). These scripts score the crossover points and potential libraries based on the identity around the crossover point, where larger numbers represent more identical residues around the crossover point (see [Materials and Methods](#) for details). As a protein scaffold for SCHEMA-RASPP calculations, we used a

homology model of OB-1 based on the high-resolution structure of *Trametes trogii* laccase (PDB entry 2HRG, with a sequence identity of 96% vs OB-1), a laccase formed by three cupredoxin  $\beta$ -barrel domains (D1, D2, and D3) that shares 96% sequence identity with OB-1. The T2/T3Cu cluster is located at the interface between D1 and D3, whereas the T1Cu site and the HisCysHis electron transfer pathway are situated in D3. The substrate binding site is formed by residues belonging to D2 and D3, and the overall structure of the enzyme is stabilized by two interdomain disulfide bridges.

Taking into account this structural information, we ran the SCHEMA-RASPP algorithm in an attempt to find crossover points between the parental laccases that minimize protein structure disruption in the resulting recombination library. We designed several computational libraries of 4 to 7 SCHEMA blocks, with ( $E$ ) ranging from 8 to 12 and ( $m$ ) from 58 to 65, [Supplementary Table S1](#). To maintain a good balance between transformation efficiency and recombination, we chose a library with 4 blocks for *in vivo* cloning in yeast (three recombination events between blocks and two to link the blocks to an expression vector). This library strikes a good balance between homology at the crossover points, modulation of the Cu binding sites and overall structural conservation. The library selected had ( $m$ ) and ( $E$ ) values of 58 and 8, respectively, with defined crossover positions at residues 168, 310, and 442 (numbered according to the mature OB-1 laccase protein: see [Figure 1](#) for a structural overview of this library). Our parent laccases contain three  $\beta$  sandwiches belonging to the corresponding cupredoxin domains. The N-terminal block 1 contains the first cupredoxin domain and the structurally



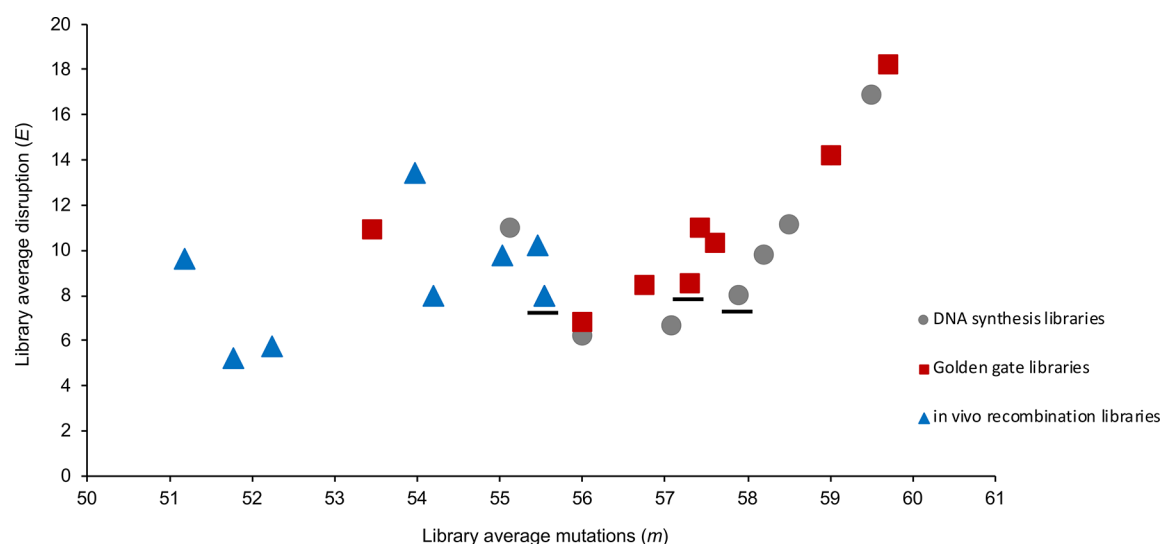


**Figure 2.** Comparison of library construction methods on SCHEMA disruption energy and mutation rate.  $E$  and  $m$  values calculated for each of 8 libraries designed for assembly through 3 different methods: *in vivo* recombination (blue triangles), golden gate assembly (red squares), and direct DNA synthesis (gray circles). Selected library used in the present study constructed by three different methods is underlined. In general, *in vivo* recombination decreases the library average number of mutations (by 4 mutations) and the disruption energy obtainable through recombination (by 1.7  $E$  values). Golden gate assembly (where the parent sequences are not mutated but the crossover points are slightly shifted away from RASPP-calculated optimal sites) slightly decreases the library average number of mutations (by 0.5 mutations) and slightly increases disruption energy (by 0.5  $E$  values). Comparative  $E$  and  $m$  values are relative to the synthetic library.

adjacent loop and  $\beta$ -strands of the second domain; block 2 contains the remainder of the second cupredoxin domain; blocks 3 and 4 make up the third cupredoxin domain, with block 4 also containing the C-terminal  $\alpha$  helix that interacts with block 1. Although the coordination spheres of both the T1Cu and T2/T3Cu cluster were not near any designed crossover point, the SCHEMA design was selected to modulate both Cu binding sites. Indeed, blocks 3 and 4 participate in the first coordination shell of the T1Cu ion, with two coordinating His and one Cys residues. The trinuclear T2/T3Cu cluster is coordinated by six His residues distributed within SCHEMA blocks 1, 3 and 4, Figure 1. Finally, the HisCysHis tripeptide, which physically connects the T1Cu ion and the T2/T3 Cu cluster, is responsible for intramolecular electron transfer and it is located in the last and smallest fragment.

When checking the multiple sequence alignment of the parental types, there appeared to be only a few regions with sufficient homology for the *in vivo* assembly of SCHEMA blocks, including the crossover point 422 between blocks 3 and 4. Despite the new SCHEMA algorithm, the sequence identity between the three laccase templates at the first two crossover locations (168 and 310 positions) was not high enough to guarantee reliable recombination events in *S. cerevisiae*, Supplementary Figure S2. Indeed, on average, 40 bp of homology at a given crossover location is necessary to facilitate the *in vivo* splicing between blocks without jeopardizing the yeast transformation efficiency, which is necessary to generate a mutant library with enough clones to screen.<sup>30</sup> Consequently, we decided to modify the parental sequences using OB-1 as a template given its higher thermostability (Table 1), such that there is 30 to 40 bp of homology at each crossover point selected by SCHEMA-RASPP, Supplementary Figure S3. For the first crossover site, only one residue in Lac3 and two residues in 3PO were substituted, whereas at the second crossover site, we needed to change three residues in Lac3 and

five in 3PO. In the third crossover site, homology between the three parents was good enough so that no further mutations were included. These parental mutations reduced the library average number of mutations introduced through chimera-genesis (the  $m$  value) to 56 and the  $E$  value remained at 8. Through this strategy, we simply transformed yeast with the pool of individual SCHEMA blocks along with the linearized plasmid.<sup>31</sup> Accordingly, one-pot repair and cloning was carried out *in vivo* to generate a complete set of laccase chimeras. The success of this cloning strategy was noteworthy, as thousands of clones per transformation reaction were recovered even though five recombination events were necessary to close the full autonomously replicating plasmid. Given that we shuffled 4 blocks between three orthologs, 81 possible hybrid clones ( $3^4$ ) can be theoretically created. In the library, this number could even be higher due to the potential of *S. cerevisiae* to shuffle DNA within SCHEMA blocks (see below). In order to validate our library construction method by *in vivo* recombination, we compared it with *in vitro* methods used in SCHEMA studies (golden gate assembly and direct DNA synthesis). Eight libraries were designed *in silico* for all the three methods aimed at assessing the effect on  $E$  and  $m$  values. As expected, when increasing the homology of the parents, both  $E$  and  $m$  slightly decreased using the *in vivo* recombination approach, Figure 2. This small decrease is compensated in terms of library creation simplicity (avoiding ligation steps), and it adds the possibility of including beneficial intrablock recombination events (see below).

**Sequence Analysis and Thermostability of Laccase Chimeras.** A general precondition for an enzyme to be exploited industrially is its thermal stability. Therefore, engineering thermostable fungal laccases with the capacity to withstand harsh industrial reaction conditions is particularly desirable.<sup>2,32</sup> In addition, such stable laccases provide promising departure points for future evolutionary endeavors, since they will be better able to tolerate destabilizing mutations

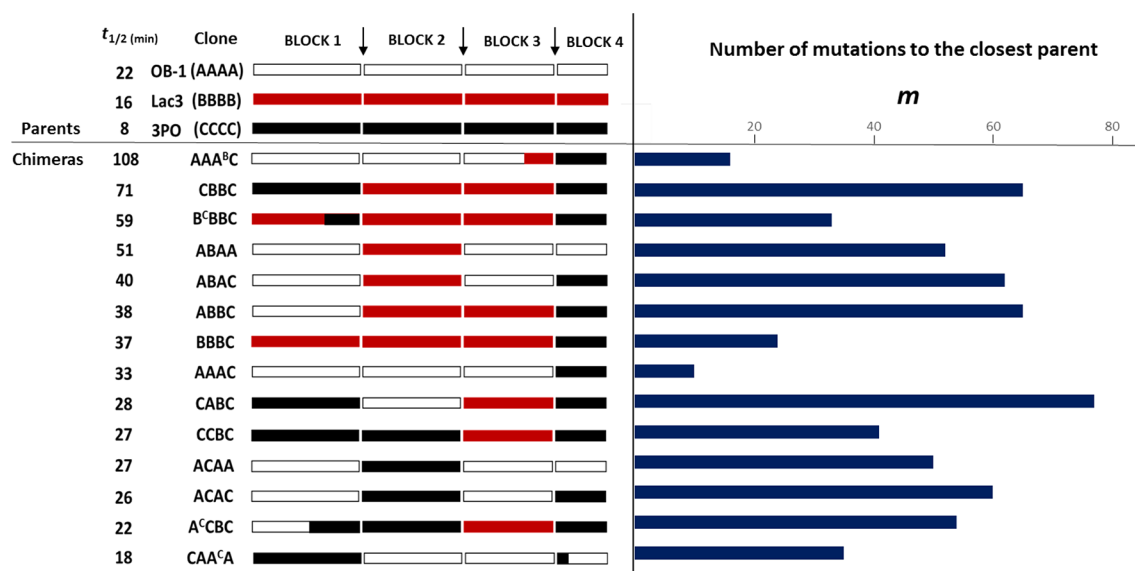


**Figure 3.** Family of thermostable chimeric laccases. Sequence diversity is highlighted by colors, where white stands for AAAA (OB-1), red for BBBB (Lac3), and black for CCCC (3PO). The blue bars show the amino acid differences between the corresponding chimera and its closest homologue. The half-life inactivation time ( $t_{1/2}$ ) of chimeric laccases at 70 °C is shown in the left column. Appropriate enzyme supernatant dilutions in 20 mM bis-tris buffer pH 6.0 were incubated at 70 °C. Aliquots (50  $\mu$ L) were removed after 5, 15, 25, 35, 55, 75, 95, and 120 min, chilled on ice for 10 min and further incubated at room temperature for at least 5 min. Subsequently, the residual activity (initial rates) was determined in an 2,2'-azino-bis(3-ethylbenzothiazoline-6-sulfonic acid) (ABTS) assay (100 mM sodium phosphate/citrate buffer pH 4.0 and 3 mM ABTS), and it was expressed relative to the ABTS activity at room temperature. Each value is the average of three independent experiments.

required for novel activities.<sup>33</sup> We screened the chimeric library for thermostability using a high-throughput assay we developed previously and applied to other fungal ligninases expressed by yeast.<sup>34</sup> Around 1000 clones were screened by measuring their residual activity after heat shock at 70 °C for 10 min. After three consecutive rescreenings, 14 unique thermostable laccase chimeras were isolated and characterized (Figure 3). This set of chimeras had high sequence diversity that varied from their closest parent by between 10 to 77 mutations. On average, 46 amino acid substitutions were introduced from the closest parent sequence and these chimeras were named according to their fragment composition: A representing SCHEMA blocks for OB-1 (AAAA), B for Lac3 (BBBB), and C for 3PO (CCCC), with noncomputed blocks indicated in superscript. Five chimeras (AAA<sup>B</sup>C, ABAC, ABBC, CABC, and A<sup>C</sup>CBC) were composed of SCHEMA blocks from all three parental types. Moreover, chimeras AAA<sup>B</sup>C and A<sup>C</sup>CBC, together with B<sup>C</sup>BBC and CAA<sup>C</sup>A, underwent further recombination within the SCHEMA blocks due to stochastic *in vivo* shuffling, thereby producing functional enrichment of the mutant library. The broad sequence diversity generated by the *in vivo* SCHEMA-RASPP guided recombination was much higher than that found in any previous attempt of laccase chimeragenesis.<sup>7–9</sup>

Of the 14 thermostable laccases identified, 12 exhibited a higher  $t_{1/2}$  of thermal inactivation at 70 °C relative to the most stable parent, OB-1 (Figure 3). Although 3PO was the least thermostable parent, when the composition of the chimeras was examined, the last block of 3PO (C4) appeared to be strongly stabilizing in this context, participating in 85% of the thermostable laccases, Supplementary Figure S4. Block 4 is the smallest of the SCHEMA blocks, representing only 11% of the protein sequence, although it does contain roughly 40% of all the  $\alpha$ -helix forming residues, which seem to be crucial for the overall protein stability. Conversely, the C3 block from 3PO

was not observed in any of the thermostable variants selected, suggesting a destabilizing effect that it may contribute to the low stability of 3PO, Supplementary Figure S4. Of all the chimeras, AAA<sup>B</sup>C showed a striking 5-fold increase in thermostability relative to the most stable parent, OB-1 (AAAA). The AAA<sup>B</sup>C chimera had a  $t_{1/2}$  of thermal inactivation at 70 °C of 108 min (77 min longer than AAAC), yet the only difference between the AAA<sup>B</sup>C and AAAC chimeras is the substitution of a 18 residue segment in block A3 from OB-1 with the final region of block B3 from Lac3. This modification was the result of an intrablock (nondesignated) *in vivo* homologous recombination, introducing six additional mutations into block 3 (relative to A3): V424T, N426S, S429T, P430D, R439T, D441N (Supplementary Figure S5). In our laccase structural model, residues Val424 and Asn426 are located near the interface of cupredoxin domains 2 and 3, Ser429 and Pro430 at the turn of a long solvent exposed loop, and Arg439 and Asp441 are solvent exposed residues near the loop between two  $\beta$ -strands and the crossover point between SCHEMA blocks 3 and 4. Neither the transferability nor the importance for the stability of this region was predicted computationally. Only the fact that we performed a DNA shuffling *in vivo* enabled the discovery of this exceptionally stable laccase chimera.

We found stabilizing relationships between clones BBBC, B<sup>C</sup>BBC, and CBBC in our chimeric collection that might also affect the patterns of activity (see below). These chimeras were comprised exclusively of Lac3 and 3PO blocks, the two least stable parents. By accumulating more of 3PO in block 1, a gradual increase in thermostability was detected, from  $t_{1/2} = 37$  min to  $t_{1/2} = 71$  min.

All three clones contained the stabilizing C4 block from 3PO, which improved BBBC clone stability 2.3-fold over the closest and most stable parent, in this case Lac3. The incorporation a 36 amino acid segment of 3PO at the end of

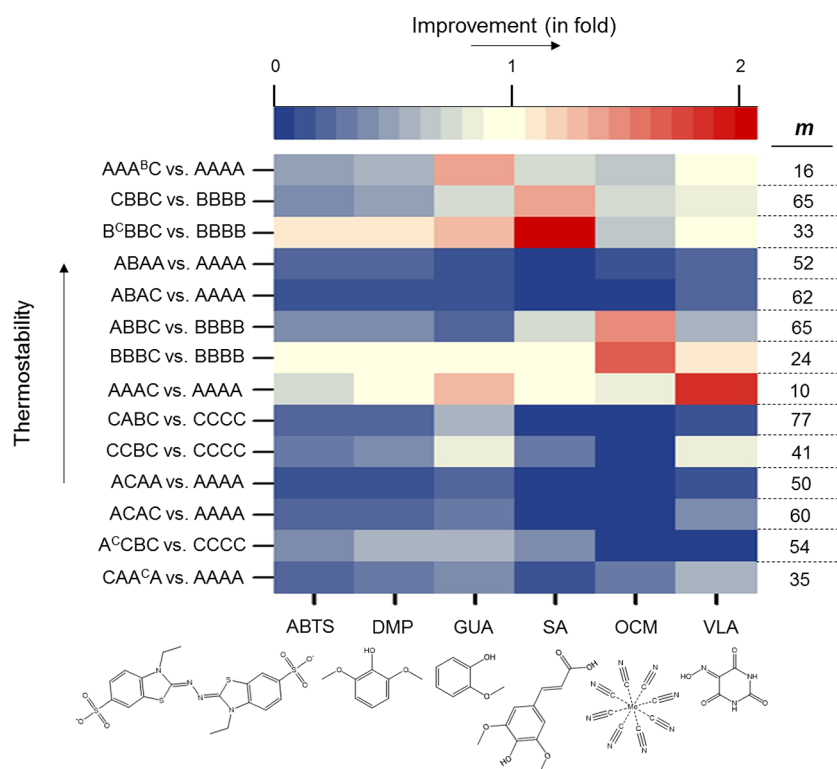


**Figure 4.** Activity of the chimeras on different substrates. Heat map of the total activity of the 14 chimeric laccases relative to the parental type. The parental type is defined as the closest homologue for each chimera and the chimeras are organized by increasing thermostability. The number of mutations relative to the closest parent ( $m$ ) is highlighted on the left column. Supernatants of the chimeras and parental types (20  $\mu$ L) were mixed with 180  $\mu$ L of 100 mM sodium phosphate/citrate buffer pH 4.0, and the corresponding substrates: 3 mM ABTS, 3 mM 2,6-dimethoxyphenol (DMP), 10 mM guaiacol (GUA), 2 mM potassium octacyanomolybdate (OCM), 0.25 mM sinapic acid (SA), and 20 mM violuric acid (VLA). The reactions were performed in triplicate, and the laccase activity was normalized to the closest parental type.

block 1 further introduced 9 mutations in the B<sup>C</sup>BBC clone resulting in an overall 3.7-fold improvement of the stability. Finally, when the whole of block 1 was swapped between Lac3 and 3PO in the CBBC chimera, we observed an overall 4.4-fold increase in thermostability. In summary, several segments of the least stable parent 3PO can positively contribute to protein stability in chimeras.

#### Activity Pattern of Thermostable Laccase Chimeras.

We assessed the preliminary oxidation capacity of thermostable chimeras using six laccase substrates of different chemical nature and redox potential. Initial rates of laccase chimeras estimated in fresh supernatants are arranged in a heat map to compare them to their closest homologue, Figure 4. Globally, many variants were found to have a total activity lower than their closest homologues, for the majority of the substrates tested (blue tints dominate the map). The C2 block clearly appears to diminish the total activity, as the four chimeras containing block 2 of 3PO acted weakly on all the substrates tested. Notably, the three most thermostable clones (AAA<sup>B</sup>C, CBBC and B<sup>C</sup>BBC) maintained or even improved their activity for some of the substrates. Chimeras BBBC and ABBC displayed  $\sim$ 1.7- and 1.5-fold enhanced activity when oxidizing the high-redox potential substrate potassium octacyanomolybdate IV (OCM, a metal transition complex used as a laccase redox mediator). Similarly, clone AAAC displayed a 1.9-fold improvement in the oxidation of another high-redox potential mediator, violuric acid (VLA). In the case of low-redox potential mediator sinapic acid (SA), the chimera B<sup>C</sup>BBC exhibited a 2-fold enhancement, while CBBC also performed 1.4-fold better than its closest parent. Curiously, we did not

detect any improvements for other low-redox potential compounds like phenolic 2,6-dimethoxyphenol (DMP), guaiacol (GUA), or the nonphenolic mediator 2,2'-azino-bis(3-ethylbenzothiazoline-6-sulfonic acid) (ABTS), although with GUA a modest increase could be observed with some variants.

To explore the activity patterns observed among the chimeric laccases, we established a structural alignment of the parental sequences surrounding the T1Cu site, Figure 5. Previously, several amino acid positions of the catalytic cavity (162–164, 205, 263, 264, 331, 336, 390–392, and 455) have been shown to influence substrate oxidation in other high-redox potential laccases sharing 96 to 98% sequence identity to OB-1.<sup>35,36</sup> Moreover, we recently enhanced the redox potential of the OB-1 laccase by computational and directed evolution methods, showing that the residue at position 458 is involved in both the binding and the redox potential of the T1Cu site (unpublished material). Interestingly, all four SCHEMA-RASPP designed blocks participated to a greater or lesser extent in sculpting the catalytic cavity of the chimeras. The 162–164 loop belongs to block 1, whereas the highly conserved Asp205 (harboring the first acceptor proton of the redox process) and the 263–264 loop are part of block 2. There are two conserved Phe at positions 331 and 336 in block 3, together with loop 390–392 in the vicinity of the T1Cu site, while the  $\alpha$  helix that carries the conserved Ala458 and His455 (the first electron acceptor) is within block 4, Figure 5. Therefore, the combination of variations in these segments could be used to rationalize the different substrate oxidation patterns observed among the chimeras.

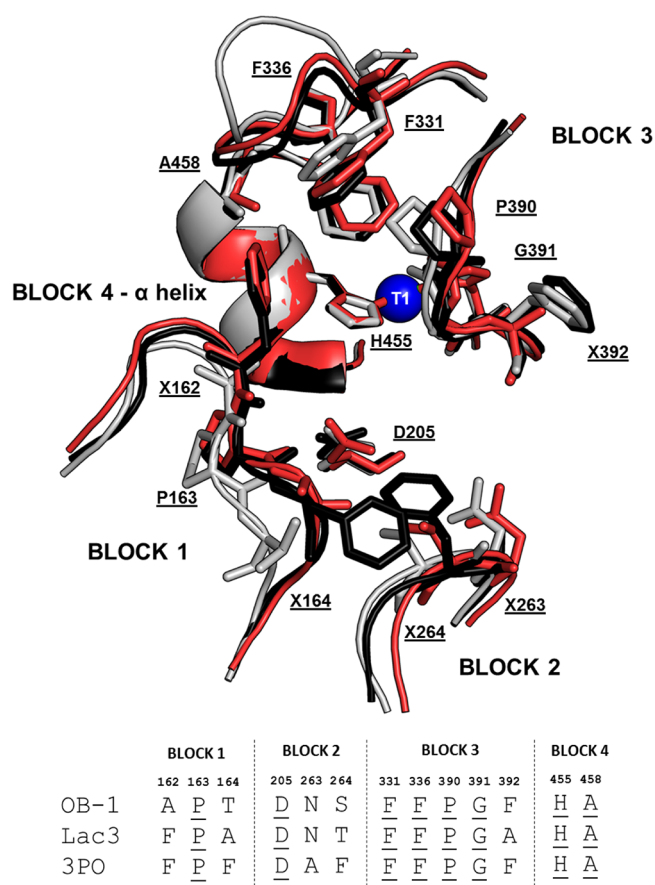


**Figure 5.** Structural alignment of the parental binding pocket sequences. The alignment is represented as a cartoon: OB-1, gray; Lac3, red; 3PO, black. Residues involved in the catalytic pocket are highlighted as sticks and the T1Cu is depicted as a blue sphere, with X defined as a variable residue. Model of the OB-1 laccase based on the high resolution structure of *Trametes trogii* laccase (PDB entry 2HRG), sharing 96% sequence identity with OB-1. Model of the Lac3 laccase based on crystal structure of *Trametes* sp. AH28–2, sharing 77% sequence identity with Lac3 (PDB entry 3KW7) and the model of 3PO laccase based on crystal structure of the Pcl (PDB entry 2XYB). The images and alignments were generated and analyzed with the PyMOL Molecular Visualization System (<http://pymol.org>).

Depending on how the SCHEMA blocks combine with each other, synergies, incompatibilities, or neutral effects on the catalytic cavity could be observed. To illustrate this, we chose clones BBBC, B<sup>C</sup>BBC, and CBBC that have very different SA or OCM oxidizing activity relative to the common closest homologue, despite only differing in block 1 (Figure 3, 4). Our structural alignment identified the 162–164 loop in block 1 as responsible for this effect, contributing to the variation in activity between the three chimeras, Supplementary Figure S6. Both B<sup>C</sup>BBC and CBBC showed enhanced oxidation of SA, in which loop 162–164 only came from 3PO, Figures 3, 4, 5. Conversely, there was no improvement in chimera BBBC, whose loop 162–164 comes from Lac3. The only difference in this loop between the three chimeras was at position 164, where there is an Ala or Phe residue from Lac3 or 3PO, respectively. Hence, the A164F substitution seems to have an important effect on the oxidation of SA. By contrast, we observed the opposite effect when comparing the oxidation of OCM by these three chimeras. Thus, while the activity of BBBC was ~1.7-fold better than that of the parental type,

B<sup>C</sup>BBC and CBBC retained only roughly 60% of this activity, highlighting the correlation between an Ala instead of a Phe at position 164 and a more efficient oxidation of OCM. Although shifting substrate specificity was not the primary goal of our screen, the different oxidation patterns found among the chimeras, along with the trade-off in activity displayed by some of the variants highlights the potential of SCHEMA-RASPP structure guided recombination *in vivo* to modulate the substrate preferences of promiscuous enzymes.

**pH Stability of Thermostable Laccase Chimeras.** In addition to elevated temperatures, industrial processes are often performed under extreme pH conditions, which may decrease the activity and stability of enzymes. Optimum pH activity of fungal laccases is generally between 2 to 5, pHs at which they are not very stable for extended periods. On the other hand, fungal laccases possess good storage stability at alkaline pH, although they do not show activity due to the reversible binding of hydroxide ions to the T2/T3 site.<sup>37</sup> Considering their stronger activity at acidic pHs, a critical aspect of laccase performance is endurance in harsh acidic conditions. In order to examine the pH stability of the chimeras, we selected the 5 most thermostable and active variants (AAA<sup>B</sup>C, CBBC, B<sup>C</sup>BBC, ABBC, and BBBC), which were incubated at different pHs and their residual ABTS activity was measured at pH 4.0. As expected, at neutral and basic pHs both the chimeras and the parental types were very stable, conserving 80–100% of residual ABTS activity, Supplementary Figure S7. With a gradual increase in the acidity of the environment, the two most thermostable chimeras (AAA<sup>B</sup>C and CBBC) displayed a significant stronger pH stability than any of the parents. After 72 h at pH 2.0, the AAA<sup>B</sup>C clone retained almost 70% of its activity, whereas the OB-1 variant, its closest parent, was practically inactive, Figure 6A. A similar effect was observed when comparing CBBC to its closest parent, Lac3, with an 8-fold improvement at pH 2.0 after 72 h, Figure 6A. Of the 3 parental types, 3PO exhibited the highest acidic pH stability, such that the increasing contribution of SCHEMA blocks from 3PO to the corresponding chimeras is beneficial to their pH stability. This is especially true for the SCHEMA block C1, which was gradually incorporated into the chimeras (from BBBC to B<sup>C</sup>BBC and finally, to CBBC), with a concomitant progressive increase of stability at pH 2.0, Figure 6B. It is noteworthy that similar influence for the C1 block was earlier evidenced in the description of the thermostabilization of these three chimeric proteins, Figure 3. Moreover, the acid stability of AAA<sup>B</sup>C and CBBC perfectly complements their remarkable thermal stability and activity, which makes them robust biocatalysts for industrial uses.

## CONCLUSION

We generated a family of thermostable chimeric laccases by SCHEMA-RASPP structure guided recombination *in vivo*, an approach not yet applied to laccase engineering. SCHEMA-designed protein blocks of three different laccases enabled chimeric laccases to be created by minimizing the disruption of the folded structure at the same time as *in vivo* shuffling, and assembly in yeast allowed recombination between and within the SCHEMA blocks, enriching the sequence and functional diversity of the chimeric library. This strategy proved to be extremely useful, to enhance not only thermal stability, but also stability at acidic pH and activity on different substrates, properties that were not under selection. By distributing



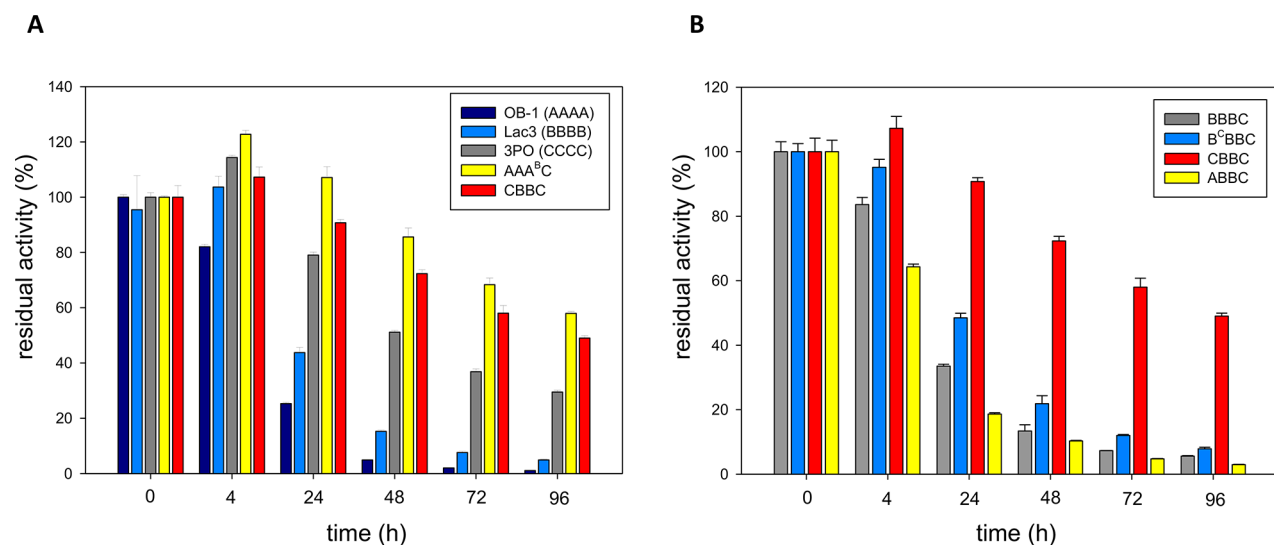


**Figure 6.** Enzyme stability at pH 2.0. (A) Comparison between the parental types and the two most stable chimeras. (B) Comparison between chimeras that only differ in block 1. Laccases variants were incubated for 0, 4, 24, 48, 72, and 96 h at pH 2.0. Residual activity after each time was measured with 3 mM ABTS in 100 mM sodium phosphate/citrate buffer pH 4.0. Laccase activity was normalized to the highest activity at time 0, and each point and standard deviation is derived from three independent measurements.

residues in different SCHEMA blocks, we managed to explore sequence-function relationships of chimeric laccases, and to identify specific residues influencing substrate oxidation. Significantly, the shuffling within blocks provided relevant information about the contribution of SCHEMA blocks to the biochemical properties of the chimeras. This collection of stable laccase chimeras represents an excellent starting point for future adaptive evolution endeavors. Given the structural complexity of laccases, the success obtained here by bringing together computational SCHEMA-RASPP and *in vivo* recombination also paves the way to engineer other structurally complex proteins.

## MATERIAL AND METHODS

**Materials.** ABTS (2,2'-azino-bis(3-ethylbenzothiazoline-6-sulfonic acid)), DMP (2,6-dimethoxyphenol), VLA (violic acid), OCM (IV potassium octacyanomolybdate), GUA (guaiacol), SA (sinapic acid), and yeast transformation kit were purchased from Sigma-Aldrich/Merck (Darmstadt, Germany). The high-fidelity DNA polymerase PfuUltra was acquired from Agilent. *S. cerevisiae* strain BJS465 was from LGC Promochem (Barcelona, Spain), while *Escherichia coli* XL2-Blue competent cells were from Stratagene (La Jolla, CA, USA). Zymoprep yeast plasmid miniprep kit and ZymoClean Gel DNA Recovery Kit were from Zymo Research (Orange, CA, USA). The NucleoSpin Plasmid kit was purchased from Macherey-Nagel (Düren, Germany). The restriction enzymes (*Bam*HI, *Xho*I) were from New England Biolabs (Hertfordshire, UK). Oligonucleotides were synthesized by Metabion (Bayern, Germany). All chemicals were reagent-grade purity.

**Culture Media.** The selective expression medium (SEM) contained filtered yeast nitrogen base (100 mL, 6.7%), filtered yeast synthetic drop-out medium supplement without uracil (100 mL, 19.2 g/L), filtered KH<sub>2</sub>PO<sub>4</sub> buffer (pH 6.0, 67 mL, 1 M), filtered galactose (111 mL, 20%), absolute ethanol (31.6 mL), filtered chloramphenicol (1 mL, 25 g/L), filtered CuSO<sub>4</sub> (1 mL, 1M), and ddH<sub>2</sub>O (to 1000 mL). Sterile minimal medium contained 100 mL 6.7% filtered yeast nitrogen base, 100 mL 19.2 g/L filtered yeast synthetic drop-out medium

supplement without uracil, 100 mL filtered 20% raffinose, 700 mL ddH<sub>2</sub>O, and 1 mL 25 g/L filtered chloramphenicol. SC drop-out plates contained 100 mL 6.7% filtered yeast nitrogen base, 100 mL 19.2 g/L filtered yeast synthetic drop-out medium supplement without uracil, 20 g autoclaved bacto agar, 100 mL 20% filtered glucose, 1 mL 25 g/L filtered chloramphenicol, and ddH<sub>2</sub>O to 1000 mL. Sterile expression medium contained 720 mL autoclaved YP, 67 mL 1 M filtered KH<sub>2</sub>PO<sub>4</sub> pH 6.0 buffer, 111 mL 20% filtered galactose, 31.6 mL absolute ethanol, 1 mL 25 g/L filtered chloramphenicol, 2 mL 1 M filtered CuSO<sub>4</sub>, and ddH<sub>2</sub>O to 1000 mL. YP medium contained 10 g yeast extract, 20 g peptone, and ddH<sub>2</sub>O to 650 mL. YPD solution contained 10 g yeast extract, 20 g peptone, 100 mL 20% sterile glucose, 1 mL 25 g/L chloramphenicol, and ddH<sub>2</sub>O to 1000 mL. Luria–Bertani (LB) medium was prepared with 5 g yeast extract, 10 g peptone, 10 g NaCl, 100 mg ampicillin, and ddH<sub>2</sub>O to 1000 mL.

**Protein Modeling.** Structural alignment of catalytic pocket residues was made using a model of OB-1 laccase based on high resolution structure of *Trametes trogii* laccase (PDB entry 2HRG),<sup>35</sup> sharing 96% sequence identity with OB-1, a model of Lac3 *Trametes* sp. laccase based on crystal structure of *Trametes* sp. AH28–2, sharing 77% sequence identity with Lac3 (PDB entry 3KW7),<sup>38</sup> and a model of 3PO laccase based on crystal structure of the Pcl (PDB entry 2XYB). Homology models were built using the SWISS-MODEL Web server.<sup>39</sup> The structural alignment and images were generated and analyzed by PyMOL Molecular Visualization System (<http://pymol.org>).

**SCHEMA-RASPP Library Design.** SCHEMA-RASPP was used to design the 4-block contiguous recombination library of the three parent laccases (OB-1, 3PO, and Lac3) that minimizes the library-average disruption of protein structure.<sup>21,40</sup> An alignment of mature parental sequences (lacking their respective signal sequences) was generated in Clustal Omega (“parental alignment”). A separate alignment of the mature OB-1 sequence with the sequence extracted from the OB-1 homology model was also generated in Clustal Omega (“PDB alignment”). The parental and PDB alignments, the



OB-1 homology model (PDB file), the desired number of crossovers ( $x_0 = 3$ ), and a minimal number of mutations per block ( $\text{min} = 20$ ) were used as inputs for SCHEMA-RASPP calculations. The RASPP output is a list of SCHEMA libraries, with each library defined by a set of cross over points and annotated with average  $E$  and  $m$  values. To facilitate homologous recombination between fragments with minimal modification of the parental sequences, we developed an additional algorithm to score each of these libraries and the corresponding crossover points for homology levels between the three parental laccases (“add\_scores” algorithm). We assessed multiple library designs by the  $E$  and  $m$  values, homology scores, and visualization on the OB-1 homology model. Ultimately we selected a library that was well balanced between homology at the crossover points, modulation of the Cu binding sites, structural conservation, a minimal number of blocks, and a minimal  $E$  value. The library design was made using software packages for calculating SCHEMA energies openly available at <http://cheme.che.caltech.edu/groups/fha/Software.htm>. The add\_scores algorithm is available in the Supporting Information.

#### Comparison of Chimera Assembly Methods on SCHEMA Disruption Energy and Mutation Rate.

RASPP curves were generated for unmutated, mature laccase sequences. Eight potential SCHEMA libraries were selected such that trivial (relatively small) blocks were not considered. One of these libraries had an excellent combination of multiple properties (see main Materials and Methods) and was ultimately assembled through homologous recombination. To facilitate homologous recombination, the parental sequences were mutated at desired crossover points to provide at least 33 bp of homology. This is expected to decrease the number of mutations possible through recombination (the  $m$  value) as well as the disruption of the chimeric protein structure relative to the parents (the  $E$  value), though the ultimate effect on the  $E$  value will depend on if the areas mutated for increased homology participate in contacts that can be disrupted through recombination. To further explore the effect of the chimera assembly method on  $m$  and  $E$  values, eight selected libraries were designed (only *in silico*) for homologous recombination, golden gate assembly, and direct DNA synthesis. For homologous recombination, 33–39 bp of homology was engineered at the crossover points indicated by the unmutated parents RASPP curve; a new parental alignment was made; SCHEMA contacts,  $E$ , and  $m$  values were calculated for each library. Note that new parents were designed for each of eight libraries. For golden gate assembly, the parents were not mutated for increased homology, but the crossover points were shifted away from the sites indicated by RASPP to the nearest site with four base pairs of homology (required by golden gate assembly). For each library,  $E$  and  $m$  values were recalculated at the new cross over points. Library generation through direct DNA synthesis represents an ideal situation that yields  $E$  and  $m$  values calculated *via* RASPP.

**Chimeric Library Creation in *S. cerevisiae*.** The parental types OB-1, 3PO and Lac3 were obtained as described elsewhere.<sup>5,6,25</sup> To allow the *in vivo* assembly of SCHEMA blocks, specific crossover events were promoted between blocks. To do so, SCHEMA blocks were amplified with primers that generate overlapping areas of ~40 bp flanking each block, Supplementary Table S2. Overlapping areas with the linearized PjRocC30 plasmid were also included to allow

the reparation of an autonomously replicating vector upon transformation in yeast.

All oligonucleotides used to amplify SCHEMA blocks are indicated in Supplementary Table S2. All 12 PCR reactions were carried out in a final volume of 50  $\mu\text{L}$  containing 3% DMSO, 0.3 mM dNTPs (0.075 mM each), 0.25  $\mu\text{M}$  of each primer, 0.05 U/ $\mu\text{L}$  PfuUltra DNA polymerase, and 2 ng/ $\mu\text{L}$  of template. PCR reactions were carried out on a gradient thermocycler using the following parameters: 95 °C for 2 min (1 cycle); 95 °C for 45 s, 50 °C for 45 s, and 72 °C for 60 s (28 cycles); and 72 °C for 10 min (1 cycle). Block 1 was amplified in 3 independent PCR reactions (1 PCR for each parental type). Details of all PCR reactions are in the Supporting Information. All PCR products were loaded onto a preparative agarose gel and purified by use of the Zymoclean Gel DNA Recovery kit. Plasmid pJRoC30 was linearized using BamHI and XhoI restriction enzymes. The linearized vector was loaded onto a preparative agarose gel and purified with the Zymoclean Gel DNA Recovery kit. All blocks were cloned into *S. cerevisiae* together with the linear plasmid and the whole genes were *in vivo* reassembled and shuffled within *S. cerevisiae* competent cells. The PCR products (12 fragments, 100 ng each) were mixed with the linearized vector (400 ng) and transformed into competent cells using the yeast transformation kit (Sigma). Transformed cells were plated in SC drop-out plates and incubated for 3 days at 30 °C. Colonies containing the whole autonomously replicating vector were picked and subjected to the screening assay.

**Thermostability Screening Assay.** The high-throughput screening assay for thermostability was adapted from Garcia-Ruiz *et al.* with some modifications.<sup>34</sup> Individual clones were picked and inoculated in sterile 96-well plates (Greiner Bio-One, GmbH, Germany), referred to as master plates, containing 200  $\mu\text{L}$  of SEM per well. In each plate, columns number 5, 6, 7 were inoculated with the corresponding parental type, and one well (H1-control) was inoculated with *S. cerevisiae* transformed with pJRoC30-MtL plasmid (laccase without activity). Plates were sealed with parafilm to prevent evaporation and incubated at 30 °C, 220 rpm, and 80% relative humidity in a humidity shaker (Minitron, Infors, Switzerland) for 3 days. The master plates were centrifuged (Eppendorf 5810R centrifuge, Germany) for 15 min at 2500g and 4 °C. Aliquots of the supernatants were transferred from the master plates to two replica plates with the aid of a liquid handler robotic station Freedom EVO (Tecan, Switzerland), 50  $\mu\text{L}$  of mixture to a thermocycler plate (Multiply PCR plate without skirt, neutral, Sarstedt, Germany) and 20  $\mu\text{L}$  to the initial activity plate. Thermocycler plates were sealed with thermoresistant film (Deltalab, Spain) and incubated at 70 °C using a thermocycler (MyCycler, Biorad, USA). Incubation took place for 10 min (so that the assessed activity was reduced 2/3 of the initial activity). Afterward, thermocycler plates were placed on ice for 10 min and further incubated for 5 min at room temperature. Twenty  $\mu\text{L}$  of supernatants were transferred from both thermocycler and initial activity plates to new plates to estimate the initial activities and residual activities values by adding 180  $\mu\text{L}$  of 100 mM citrate phosphate buffer pH 4.0 containing 1 mM ABTS. Plates were stirred briefly and the absorption at 418 nm ( $\epsilon_{\text{ABTS}} \bullet + = 36\,000\text{ M}^{-1}\text{ cm}^{-1}$ ) was followed in kinetic mode (initial turnover rates) in the plate reader (SPECTRAMax Plus 384, Molecular Devices, Sunnyvale, CA). The same experiment was performed for both the initial activity plate and residual activity plate. The values were

normalized against the OB-1 parental type (the most thermostable one) of the corresponding plate and selected variants came from the ratio between residual activities and initial activities values. To rule out the selection of false positives, three rescreenings were carried out as described before.<sup>34</sup>

**Production of Chimeras.** For each selected chimera, cell pellets were resuspended by pipetting up and down and stirring. Twenty  $\mu\text{L}$  of resuspended mixture was transferred to 3 mL of minimal medium. After 48 h at 30 °C and 220 rpm, plasmids were extracted by Zymoprep. *E. coli* XL2-Blue were transformed with the Zymoprep product, plated into LB-amp agar plates and grown at overnight at 37 °C. Single colonies were inoculated in 5 mL LB-amp medium and were grown at 37 °C overnight. Plasmids were extracted, transformed into *S. cerevisiae* cells and plated on SC drop-out plates. After 3 days at 30 °C, single colonies were inoculated in 5 mL of minimal medium and incubated for 72 h at 30 °C and 220 rpm. Clones were refreshed in a final volume of 5 mL minimal medium with an optical density  $\text{OD}_{600} = 0.3$ . After 6–8 h of growing ( $\text{OD}_{600} = 1–1.5$ ), 9 mL of expression medium were inoculated with 1 mL preculture and incubated 48h at 30 °C and 250 rpm in a 100 mL flask. Growth and expression were followed by measuring the  $\text{OD}_{600}$  of the cultures and the activity against ABTS, as described below, until reaching the stationary phase. Cells were removed by centrifugation at 3500 rpm and 4 °C during 15 min, saving the supernatant for the activity and stability assays.

**Kinetic Thermostability.** The thermostability of the different laccase samples was estimated by assessing their half-life of inactivation time ( $t_{1/2}$ ) values using 96/384 well gradient thermocyclers. Appropriate dilutions of enzymes supernatants in 20 mM bis-tris buffer pH 6.0 were incubated at 70 °C. Aliquots of 50  $\mu\text{L}$  were removed after 5, 15, 25, 35, 55, 75, 95, and 120 min, chilled out on ice for 10 min and further incubated at room temperature at least for 5 min. Afterward, residual activity was determined in kinetic mode following the ABTS assay described above (100 mM sodium phosphate/citrate buffer pH 4.0, 3 mM ABTS). Each point and standard deviation are from three independent measurements. The half-life ( $t_{1/2}$ ) was defined as the time required by the enzyme—after incubation at 70 °C—to lose 50% of its initial activity at room temperature.

**pH Stability Measurements.** Supernatants of parental types and selected chimeras were incubated at different pH (2–9). After incubation (0, 4, 24, 48, 72, 96 h), residual activity was measured with 3 mM ABTS in 100 mM sodium phosphate/citrate buffer pH 4.0. Laccase activity was normalized to the activity value at time = 0 for highest activity obtained. Each point and standard deviation is from three independent measurements.

**Activity Assays with Different Substrates.** Twenty  $\mu\text{L}$  of chimeras and parental types supernatants were mixed with 180  $\mu\text{L}$  of 100 mM sodium phosphate/citrate buffer pH 4.0 and the corresponding substrates (3 mM ABTS, 3 mM DMP, 10 mM GUA, 2 mM OCM, 0.25 mM SA, and 20 mM VLA). Reactions were performed in triplicate, and substrate oxidations were followed through spectrophotometric changes:  $\epsilon_{418}\text{ABTS} = 36\,000\ \text{M}^{-1}\ \text{cm}^{-1}$ ;  $\epsilon_{469}\text{DMP} = 27\,500\ \text{M}^{-1}\ \text{cm}^{-1}$ ;  $\epsilon_{465}\text{GUA} = 12\,100\ \text{M}^{-1}\ \text{cm}^{-1}$ ;  $\epsilon_{388}\text{OCM} = 1460\ \text{M}^{-1}\ \text{cm}^{-1}$ ;  $\epsilon_{512}\text{SA} = 14\,066\ \text{M}^{-1}\ \text{cm}^{-1}$ ;  $\epsilon_{515}\text{VLA} = 98\ \text{M}^{-1}\ \text{cm}^{-1}$ . Laccase activity was normalized to the closest parental type.

**DNA Sequencing.** Laccase genes were sequenced by GATC-Biotech. The primers used were RMLN, FS (5'-ACGACTTCCAGGTCCTGACCAAGC-3'), RS (5'-TCAATGTCCGCGTTTCGAGGGA-3'), and RMLC (see Supplementary Table S2).

## ■ ASSOCIATED CONTENT

### 📄 Supporting Information

The Supporting Information is available free of charge on the ACS Publications website at DOI: 10.1021/acssynbio.8b00509.

Figures S1–S7, Tables S1–S2, and Supporting Methods (SCHEMA-RASPP scripts and details of PCR reactions) (PDF)

## ■ AUTHOR INFORMATION

### Corresponding Author

\*E-mail: malcalde@icp.csic.es.

### ORCID

Miguel Alcalde: 0000-0001-6780-7616

### Notes

The authors declare no competing financial interest.

## ■ ACKNOWLEDGMENTS

We truly thank Prof. Frances H. Arnold (California Institute of Technology) for her guidance and support throughout this study. This work was funded by the European Union (Bioenergy-FP7-PEOPLE-2013-ITN-607793), the CSIC (project PIE-201580E042), and the Spanish Ministry of Economy, Industry and Competitiveness (projects BIO2013-43407-R.DEWRY and BIO2016-79106-R. LIGNOLUTION).

## ■ REFERENCES

- (1) Rodgers, C. J., Blanford, C. F., Giddens, S. R., Skamnioti, P., Armstrong, F. A., and Gurr, S. J. (2010) Designer laccases: a vogue for high-potential fungal enzymes? *Trends Biotechnol.* 28, 63–72.
- (2) Mate, D. M., and Alcalde, M. (2017) Laccase: a multi-purpose biocatalyst at the forefront of biotechnology. *Microb. Biotechnol.* 10, 1457–1467.
- (3) Kunamneni, A., Camarero, S., García-Burgos, C., Plou, F. J., Ballesteros, A., and Alcalde, M. (2008) Engineering and applications of fungal laccases for organic synthesis. *Microb. Cell Fact.* 7, 32.
- (4) Mate, D. M., and Alcalde, M. (2015) Laccase engineering: from rational design to directed evolution. *Biotechnol. Adv.* 33, 25–40.
- (5) Mate, D., García-Burgos, C., García-Ruiz, E., Ballesteros, A. O., Camarero, S., and Alcalde, M. (2010) Laboratory evolution of high-redox potential laccases. *Chem. Biol.* 17, 1030–1041.
- (6) Camarero, S., Pardo, I., Cañas, A. I., Molina, P., Record, E., Martínez, A., Martínez, M. J., and Alcalde, M. (2012) Engineering platforms for the directed evolution of laccase from *Pycnoporus cinnabarinus*. *Appl. Environ. Microbiol.* 78, 1370–1384.
- (7) Pardo, I., Vicente, A. I., Mate, D. M., Alcalde, M., and Camarero, S. (2012) Development of chimeric laccases by directed evolution. *Biotechnol. Bioeng.* 109, 2978–2986.
- (8) Cusano, A. M., Mekmouche, Y., Meglecz, E., and Tron, T. (2009) Plasticity of laccase generated by homeologous recombination in yeast. *FEBS J.* 276, 5471–5480.
- (9) Nakagawa, Y., Sakamoto, Y., Kikuchi, S., Sato, T., and Yano, A. (2010) A chimeric laccase with hybrid properties of the parental *Lentinula edodes* laccases. *Microbiol. Res.* 165, 392–401.
- (10) Alcalde, M. (2007) Laccases: biological functions, molecular structure and industrial applications, In *Industrial Enzymes* (Polaina, J., and MacCabe, A. P., Eds.) pp 461–476, Springer, Dordrecht.

- (11) Jones, S. M., and Solomon, E. I. (2015) Electron transfer and reaction mechanism of laccases. *Cell. Mol. Life Sci.* 72, 869–883.
- (12) Otey, C. R., Silberg, J. J., Voigt, C. A., Endelman, J. B., Bandara, G., and Arnold, F. H. (2004) Functional evolution and structural conservation in chimeric cytochromes P450. *Chem. Biol.* 11, 309–318.
- (13) Meyer, M. M., Hochrein, L., and Arnold, F. H. (2006) Structure-guided SCHEMA recombination of distantly related  $\beta$ -lactamases. *Protein Eng., Des. Sel.* 19, 563–570.
- (14) Otey, C. R., Landwehr, M., Endelman, J. B., Hiraga, K., Bloom, J. D., and Arnold, F. H. (2006) Structure-Guided Recombination Creates an Artificial Family of Cytochromes P450. *PLoS Biol.* 4, e112.
- (15) Li, Y., Drummond, D. A., Sawayama, A. M., Snow, C. D., Bloom, J. D., and Arnold, F. H. (2007) A diverse family of thermostable cytochrome P450s created by recombination of stabilizing fragments. *Nat. Biotechnol.* 25, 1051.
- (16) Heinzelman, P., Snow, C. D., Wu, L., Nguyen, C., Villalobos, A., Govindarajan, S., Minshull, J., and Arnold, F. H. (2009) A family of thermostable fungal cellulases created by structure-guided recombination. *Proc. Natl. Acad. Sci. U. S. A.* 106, 5610–5615.
- (17) Heinzelman, P., Komor, R., Kanaan, A., Romero, P., Yu, X., Mohler, S., Snow, C., and Arnold, F. (2010) Efficient screening of fungal cellobiohydrolase class I enzymes for thermostabilizing sequence blocks by SCHEMA structure-guided recombination. *Protein Eng., Des. Sel.* 23, 871–880.
- (18) Romero, P. A., Stone, E., Lamb, C., Chantranupong, L., Krause, A., Miklos, A., Hughes, R. A., Fechtel, B., Ellington, A. D., Arnold, F. H., and Georgiou, G. (2012) SCHEMA Designed Variants of Human Arginase I & II Reveal Sequence Elements Important to Stability and Catalysis. *ACS Synth. Biol.* 1, 221–228.
- (19) Smith, M. A., Rentmeister, A., Snow, C. D., Wu, T., Farrow, M. F., Mingardon, F., and Arnold, F. H. (2012) A diverse set of family 48 bacterial glycoside hydrolase cellulases created by structure-guided recombination. *FEBS J.* 279, 4453–4465.
- (20) Bedbrook, C. N., Rice, A. J., Yang, K. K., Ding, X., Chen, S., LeProust, E. M., Gradinaru, V., and Arnold, F. H. (2017) Structure-guided SCHEMA recombination generates diverse chimeric channelrhodopsins. *Proc. Natl. Acad. Sci. U. S. A.* 114, E2624.
- (21) Voigt, C. A., Martinez, C., Wang, Z.-G., Mayo, S. L., and Arnold, F. H. (2002) Protein building blocks preserved by recombination. *Nat. Struct. Biol.* 9, 553.
- (22) Endelman, J. B., Silberg, J. J., Wang, Z.-G., and Arnold, F. H. (2004) Site-directed protein recombination as a shortest-path problem. *Protein Eng., Des. Sel.* 17, 589–594.
- (23) Alcalde, M. (2015) Engineering the ligninolytic enzyme consortium. *Trends Biotechnol.* 33, 155–162.
- (24) Klonowska, A., Gaudin, C., Asso, M., Fournel, A., Réglie, M., and Tron, T. (2005) LAC3, a new low redox potential laccase from *Trametes* sp. strain C30 obtained as a recombinant protein in yeast. *Enzyme Microb. Technol.* 36, 34–41.
- (25) Mateljak, I., Tron, T., and Alcalde, M. (2017) Evolved  $\alpha$ -factor prepro-leaders for directed laccase evolution in *Saccharomyces cerevisiae*. *Microb. Biotechnol.* 10, 1830–1836.
- (26) Heinzelman, P., Romero, P. A., and Arnold, F. H. (2013) Efficient sampling of SCHEMA chimera families to identify useful sequence elements, In *Methods in Enzymology* (Keating, A. E., Ed.), pp 351–368, Elsevier.
- (27) Farrow, M. F., and Arnold, F. H. (2010) Combinatorial recombination of gene fragments to construct a library of chimeras. *Curr. Protoc. Protein Sci.* 62, 26.2.1–26.2.20.
- (28) Mate, D. M., Gonzalez-Perez, D., Mateljak, I., de Santos, P. G., Vicente, A. I., and Alcalde, M. (2017) The pocket manual of directed evolution: Tips and tricks, In *Biotechnology of Microbial Enzymes* (Brahmachari, G., Ed.), pp 185–213, Elsevier.
- (29) Molina-Espeja, P., Viña-Gonzalez, J., Gomez-Fernandez, B. J., Martin-Diaz, J., Garcia-Ruiz, E., and Alcalde, M. (2016) Beyond the outer limits of nature by directed evolution. *Biotechnol. Adv.* 34, 754–767.
- (30) Gonzalez-Perez, D., Garcia-Ruiz, E., and Alcalde, M. (2012) *Saccharomyces cerevisiae* in directed evolution: An efficient tool to improve enzymes. *Bioengineered* 3 (3), 172–177.
- (31) Alcalde, M. (2010) Mutagenesis protocols in *Saccharomyces cerevisiae* by *in vivo* overlap extension, In *In Vitro Mutagenesis Protocols* (Braman, J., Ed.), pp 3–14, Humana Press, Totowa, NJ.
- (32) Hildén, K., Hakala, T. K., and Lundell, T. (2009) Thermotolerant and thermostable laccases. *Biotechnol. Lett.* 31, 1117.
- (33) Bloom, J. D., Labthavikul, S. T., Otey, C. R., and Arnold, F. H. (2006) Protein stability promotes evolvability. *Proc. Natl. Acad. Sci. U. S. A.* 103, 5869–5874.
- (34) García-Ruiz, E., Maté, D., Ballesteros, A., Martínez, A. T., and Alcalde, M. (2010) Evolving thermostability in mutant libraries of ligninolytic oxidoreductases expressed in yeast. *Microb. Cell Fact.* 9, 17.
- (35) Matera, I., Gullotto, A., Tilli, S., Ferraroni, M., Scozzafava, A., and Briganti, F. (2008) Crystal structure of the blue multicopper oxidase from the white-rot fungus *Trametes trogii* complexed with p-toluolate. *Inorg. Chim. Acta* 361, 4129–4137.
- (36) Pardo, I., Santiago, G., Gentili, P., Lucas, F., Monza, E., Medrano, F. J., Galli, C., Martínez, A. T., Guallar, V., and Camarero, S. (2016) Re-designing the substrate binding pocket of laccase for enhanced oxidation of sinapic acid. *Catal. Sci. Technol.* 6, 3900–3910.
- (37) Torres-Salas, P., Mate, D. M., Ghazi, I., Plou, F. J., Ballesteros, A. O., and Alcalde, M. (2013) Widening the pH Activity Profile of a Fungal Laccase by Directed Evolution. *ChemBioChem* 14, 934–937.
- (38) Ge, H., Gao, Y., Hong, Y., Zhang, M., Xiao, Y., Teng, M., and Niu, L. (2010) Structure of native laccase B from *Trametes* sp. AH28–2. *Acta Crystallogr., Sect. F: Struct. Biol. Cryst. Commun.* 66, 254–258.
- (39) Waterhouse, A., Bertoni, M., Bienert, S., Studer, G., Tauriello, G., Gumienny, R., Heer, F. T., de Beer, T. A. P., Rempfer, C., Bordoli, L., Lepore, R., and Schwede, T. (2018) SWISS-MODEL: homology modelling of protein structures and complexes. *Nucleic Acids Res.* 46, W296–W303.
- (40) Smith, M. A., and Arnold, F. H. (2014) Designing libraries of chimeric proteins using SCHEMA recombination and RASPP, In *Directed Evolution Library Creation. Methods in Molecular Biology, Methods and Protocols* (Gillam, E., Copp, J., and Ackerley, D., Eds.), pp 335–343, Springer, New York.